Interstitial Hyperthermia by Radiofrequency Needle Electrode System: Phantom and Canine Brain Studies

Hyung Sik Lee M.D., Sung Sil Chu Ph.D., Jin Sil Sung M.D.
Chang Ok Suh M.D., Gwi Eon Kim M.D., John Juhn Kyu Loh M.D.
Young Soo Kim M.D.,* Sun Ho Kim M.D.,* Sang Sup Chung M.D.*
Eun Kyung Han M.D.** and Tae Seung Kim M.D.**

Department of Radiation Oncology, Neurosurgery, and Pathology** Yonsei University College of Medicine, Seoul, Korea*

An interstitial radiofrequency needle electrode system was constructed for interstitial heating of brain tissue. Radiofrequency electrodes with Thermotron RF 8 were tested in an agar phantom and in a normal canine brain to determine how variations in physical factors affected temperature distributions. Temperature distributions were checked after heating with 1 mm diameter needle electrode implants on the corners of 1 and 2 cm squares in a phantom and plot isotherms for various electrodes arrangement. We observed that the 1 cm square array would heat a volume with a 1.25 cm radius circular field cross section to therapeutic temperatures (90% relative SAR using Tm) and the 2 cm square array with a 1.75 cm radius rectangular field with central inhomogeneity. With 2 cm long electrode implants, we observed that the 1 cm square array would heat a 3 cm long sagittal section to therapeutic temperature (90% relative SAR using Tm). We found that radiofrequency electrodes could be selected to match the length of the heating area without affecting its performance. The histopathological changes associated with RF heating of normal canine brains have been correlated with thermal distributions. RF needle electrode heating was applied for 50 min to generate tissue temperatures of 43°C.

We obtained a quarter of the heated tissue material immediately after heating and sacrificed at intervals from 7~30 days. The acute stage (immediately after heating) was demonstrated by liquefactive necrosis, pyknosis of neuronal element in the gray matter and by some polymorphonuclear leukocytes infiltration. The appearance of lipid-laden macrophages surrounding the area of liquefaction necrosis was demonstrated in all three sacrificed dogs. Mild gliosis occurring around the necrosis was demonstrated in the last sacrificed (Days 30) canine brain.

Key Words: RF interstitial hyperthermia, Normal canine brain

INTRODUCTION

In recent years, there has been increased interest in the treatment of cancer with hyperthermia, primarily as an adjuvant to radiation and brachytherapy. A tremendous effort has been continued to design hyperthermia systems that will bring the entire tumor volume to temperatures without overheating normal tissues. As a result, a number of groups that have been considering interstitial techniques for hyperthermia[1,4,5]. Since interstitial radiotherapy is commonly used for treating both superficial and deep seated tumors, interstitial hyperthermia can be given as an adjuvant treatment to the radiation therapy. Presently three methods for producing interstitial hyperthermia are being used clinically or are under investigation. These methods are RF needle electrodes, coaxial microwave antennas and ferromagnetic seeds[7,8].

One of the promising techniques is the application of a radiofrequency voltage to an array of electrodes inserted directly into the tumor. In this modality small implants about a millimeter in diameter are inserted in some type of array in the tumor volume, either percutaneously or at the time of surgery. By applying a voltage between the needles, an RF current is induced in the tissue, resulting in joule heating. In this paper, we intended to show the temperature distributions for an array of such needles in a tissue equivalent phantom model and to determine the sequential neuropathological changes that occur as a function of heat damage

*연세대학교 의과대학 의학학술연구비에 의하여 이루어졌음(1991).

over time in normal canine brain tissue.

MATERIALS AND METHODS

1. Heating Device and Temperature Measurement

The system consists of an RF generator, operating in the frequency of 8 MHz (Thermotron 8, Yamamoto Vinyter Co.), which applies a voltage between the two planes of needles. We used 1 mm diameter of needle electrodes; 1, 2, 3, 4 and 5 cm in lengths. A built-in thermometry system with five Teflon-coated probes of copper-constantan microthermocouples (Sensortek Inc., Type It-18) were also included. Block diagram is shown in Fig. 1.

2. Phantom Study

Hexadral phantoms with a thickness of 14 cm were made of 4% agar gel containing 0.2% NaCl with 0.1% NaN_3 as a preservative. Several 18-gauge catheter tubes were inserted into the phantoms from the side, and the thermocouples were placed in the tubes. During heating, the temperature in the phantoms was continuously monitored with the thermoprobes which were previously inserted into the phantoms. Just before the heating was finished, the temperature distributions in the phantoms were determined by moving the thermocouples through the catheter step by step at 0.5 cm intervals along the track. Thermograms were also taken to obtain a picture of the thermal distribution in an entire heating volume using a thermal video system (TVS-3300 ME, Nippon Avionics Co., Ltd)

Temperature distributions were checked with four 1 mm diameter needle electrode implants at 1, 2 and 3 cm squares with several lengths in a phantom model and plot isotherms after 50 min of heating with various electrode arrays.

3. Thermal Distribution Measurements in Agar Phantom

The maximum temperature at the electrodes is assumed to be held at some value, Tm[1]. The isotherms are plotted for each 0.1 Tm rise above baseline. Since the bioheat equation is linear, this means the results may be scaled to any value of Tm which is of interest. However, in order to estimate the shapes and dimensions of the regions that are heated to therapeutic temperatures, the following assumptions are made:

1) The baseline or core temperature is 20°C; 2) the maximum temperature allowed in the tumor volume is 44°C; therefore, Tm=24°C; 3) the temperature rise required in the tumor to get a therapeutic effect is 21.5°C(phantom temperature of 41.5°C); this corresponds to a temperature rise of approximately 0.9 Tm. Therefore, regions where the temperature rise is greater than 0.9 Tm are determined to illustrate the "therapeutic" region.

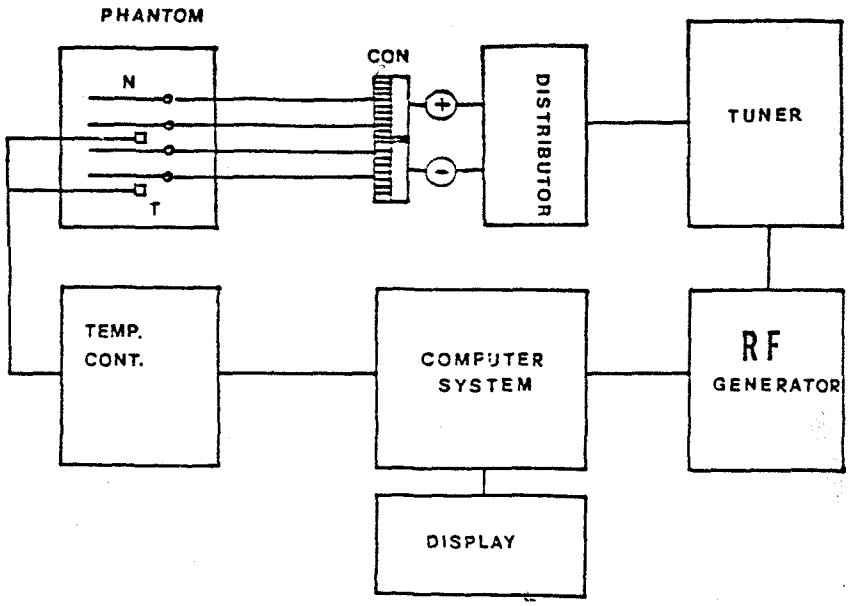

Fig. 1. Block diagram of RF induced needle electrode interstital hyperthermia system.

One sensor was placed in an area expected to achieve the highest temperature. This sensor was designated as the controller and the computer feedback system adjusted the RF wave power automatically to maintain the area adjacent to that sensor at a preselected target temperature. Once target temperature equilibrium on the control sensor was achieved (approximately 3 minutes after power was applied), the remainder of the sensors were incremented along the catheters to measure the distribution of temperature throughout the phantom.

4. Hyperthermia on Canine Brain

Dogs were anesthetized with an intravenous injection of sodium pentobarbital (50 mg/kg) and maintained in deep anesthesia with supplemental intravenous doses as required. Once fully anesthetized, dogs were placed in a frame to immobilize them to allow proper positioning of the cranium for surgical and experimental procedures. Each canine shaved head was prepared for 5 min with sterile saline/betadine solution and aseptically drapped. A midline scalp incision was made from the frontal sinus to the occipital crest and the left temporalis muscle was reflected laterally. A 4×4 cm craniotomy was made in the skull over the temporal-parietal lobes to expose the dural space. Radiofrequency needle electrodes were spaced in a 1 cm square array using constructed frame for parallel array. Thermocouples were used to measure temperature distributions in this experiment. Hyperthermic fields were generated using a needle electrode with a radiofrequency of 8 MHz (Thermotron RF 8, Yamamoto Co). Heating was carried out for 50 min at varying power intensities (average 8-12W) generating a temperature of 43°C. A sensor was located near the area expected to reach the highest temperature (center of the 1 cm square array).

Steady-state temperatures were reached in the tissue within 5 min after power initiation. After 20 min the thermocouples were withdrawn in 0.5 cm increments at 5-min intervals to map the temperature fields. After 50 min of heating, the temperature values were recorded and a quarter cm square of heated brain tissue material was obtained; thereafter, the surgical wound was sutured in layers. Antibiotics were administered prophylactically to guard against infection. The animals were mobile and fully alert within 6~10 hours post-treatment.

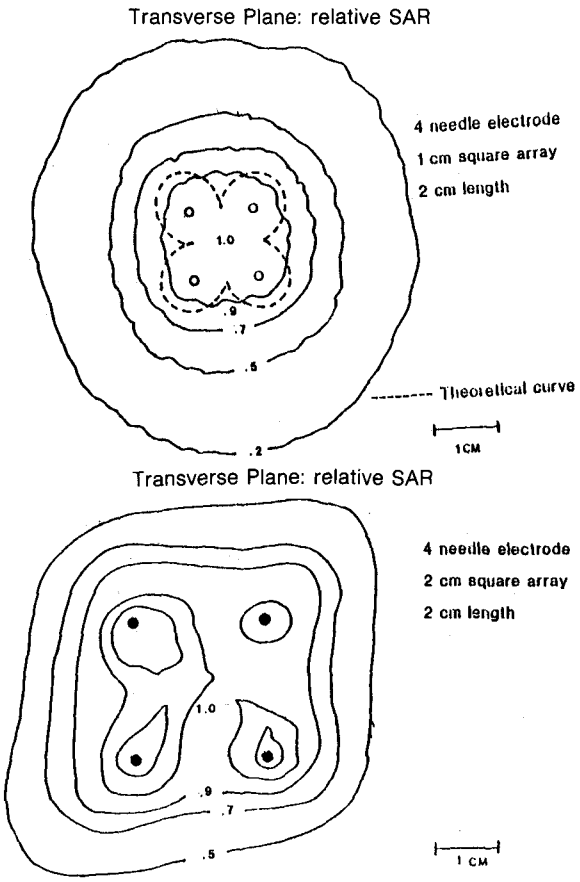

Fig. 2. Thermal distribution produced by 1 cm and 2 cm square needle electrode array: Transverse plane.

5. Pathology

Dogs were observed daily for signs of infection or neurological distress until the predetermined day of termination. The following days were chosen for histological evaluation: 0, 7, 14, 30 days. Day 0 was arbitrarily defined as the treatment day. Day 0 pathologic findings were substituted by tissue materials obtained at posthyperthermic brain field. The dogs were sacrificed and the brains were immediately removed and stored in fixative solution (1% buffered formalin) for 3 weeks. At this time, serial coronal sections were cut and photographed for gross pathological analysis.

6. Pathologic Findings

Pathological changes and thermal lesions could be easily seen on gross examination. Tissue damage associated with mechanical insertion was evaluated in each experiment. Results indicated

unremarkable pathological damage to the implanted tissue.

RESULT

1. Distribution of Temperature in an Agar Phantom

The temperature distribution (relative SAR using Tm) within agar phantom for the four 1 cm square RF needle electrode array is shown. Fig. 2 displays the transverse plane for 1 cm and 2 cm square array. In the 1 cm square array, the 90% relative SAR thermal distribution appeared homogenously as circles forming around 1.25 cm radius. With this electrode spacing the maximum relative SAR was found at the center (central axis) of the array. The right side of Fig. 2 shows the transverse plane for 2 cm square array. In this plane the 90% relative SAR isothermal curves appear homogenously as a rectangular shape with 1.75 cm radius. With this electrode spacing the maximum relative SAR was found inhomogenously at the central axis of the array. We analysed this phenomenon due to poor eletrical conductivity as the increased electrode spacing. In the sagittal plane homogenous 90% relative SAR thermal distribution was shown along the needle electrode(Fig. 3). With 2 cm length needle electrode spacing the 90% relative SAR was found at the central axis of the plane forming homogenous ellipsoid with 3 cm length. (In the historical review of microwave heating thermal curve, approximately 1.7 cm therapeutic length was shown). The right side of Fig. 3 diagrams the array as it appear from the side along its central axis (axial plane).

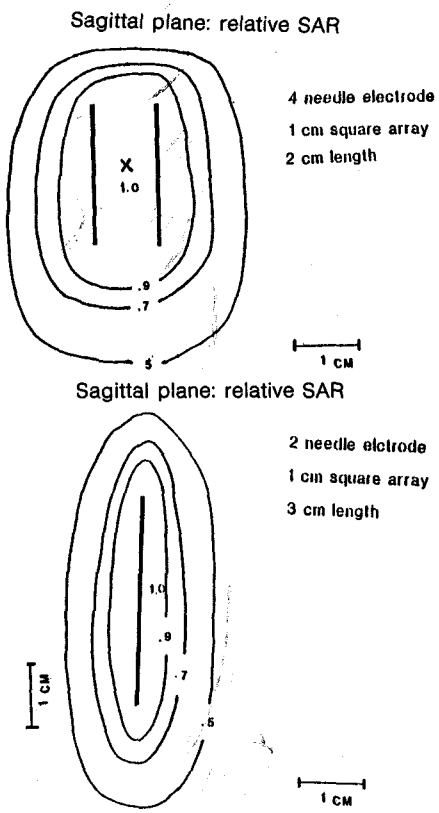

Fig. 3. Thermal distribution produced by 1 cm square array with 2 cm and 3 cm length: Sagittal plane.

Above results are plotted in Fig. 4 schematically. The geometry of implantation is critical because the electrodes must be perfectly parallel and the distance between electrodes must be suitable for hyperthermal homogeneity.

2. Pathological Findings in Canine Brain

Pathological changes and thermal lesions could be easily seen on gross examination(Fig. 5). Thermally damaged brains, depending on the stage of repair, were slightly edematous and swollen on the treated hemisphere. The hisological findings varied from on the treated hemisphere. The histological findings varied from no apparent changes by light microscopy to areas of liquefaction necrosis with and without reactive changes. For ease of description, microscopic changes in the heated tissue were assigned to three categories: (1) acute stage, (2) subacute stage and (3) chronic stage. These pathological stages are defined as follows: Acute (immediately after heating and sacrificed on day 3): Liquefactive necrosis was characterized with pyknosis of neuronal element in the gray mater and some polymorphonuclear leukocytes infiltration. Lipid-laden macrophages and perivascular lymphocytic imflammatory infiltration with vascular proliferation were also found in the sacrificed canine brain on day 3; Subacute (sacrificed on day 14): Significant reduction in the amount of cerebral edema and mass effect was observed during this stage. Lipid-laden macrophages throughout the area of brain necrosis with a margin of proliferating fibroblasts (Fig. 6). Chronic (sacrificed on day 30): Mild gliosis in the surrounding viable brain tissue was noted. Vascular proliferation was not as prominent in this stage as in the acute stage.

Although hemorrhage was not a significant finding in these experiments, the tissue changes due to thermal injury are analogous to the changes seen in cerebral necrosis due to any cause.

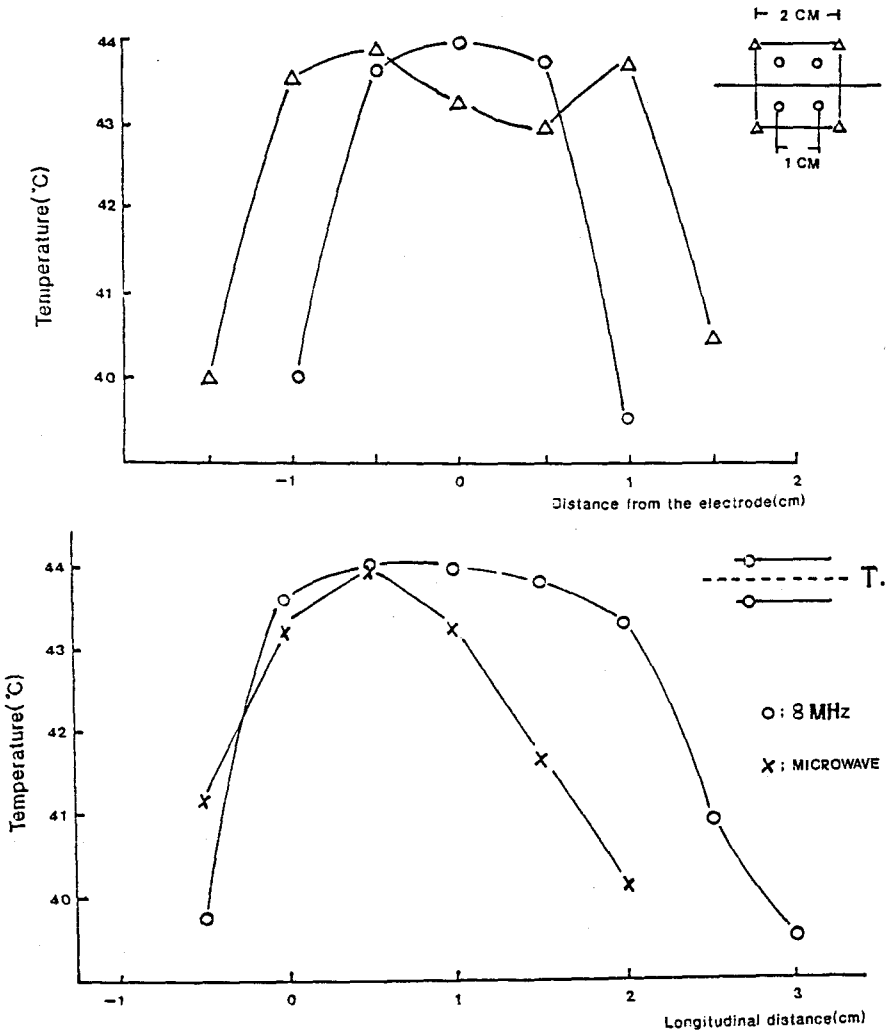

Fig. 4. Thermal plotting with transverse and longitudinal distance from needle electrode produced by 1 cm and 2 cm square, 2 cm length electrode.

DISCUSSION

The rationale for the use of hyperthermia in the treatment of human malignancies is based on a spectrum of biologic and physical research, much of the evidence accumulated over the past fifteen years. Hyperthermia is known to be cytotoxic at temperatures above 41°C. It may be lethal to cancer cells, is selectively lethal to radiation resistant cells such as S phase cells and hypoxic cells which are also at subnormal pH, is synergistic with radiation and some drugs, in part by inhibiting cellular repair systems[2~4]. It is also a physical agent, can be localized in a way similar to ionizing radiation and has tissue specific actions due to tissue specific theraml and electrical properties. Any of these factors are potentially exploitable in the clinical application of hyperthermia and are the basis for utilizing hyperthermia as an adjuvant to radiation and chemotherapy.

There are a number of groups that have been considering interstitial tchniques for hyperthermia[1,4,5]. One of the promising technique is the application of an RF voltage to an array inserted as the first step in a brachytherapy procedure.

1. Distribution of Temperature in an Agar Phantom by RF Needle Implantation

Gerner et al published the first papers of which this author is aware suggesting the implantation of RF needle electrodes to poroduce local hyperthermia[9]. Conceptually the technique is similar to producing hyperthermia using capacitive plates externally across a limb or other part of the anatomy. In capacitive plate heating an alternating RF voltage between the two capacitor plates produces a resistive current in the tissue which gives rise to joule heating. In interstitial RF hyperthermia, the implantation of two planes of needles replaces the capacitor plates. Applying a RF voltage between the two planes of needles corresponds to applying a voltage between the two capacitor plates. This RF voltage will create resistive currents between the two planes of needles, which will also heat the tissue. Since the needles can be implanted directly in, or just outside of the tumor volume, there is a good control of the power deposition and hence good control of the temperature in the tumor with less concern about the overheating normal tissue than with noninvasive systems. In addition, since the hollow needles used permit the insertion of thermometry probes and radioactive sources for brachytherapy.

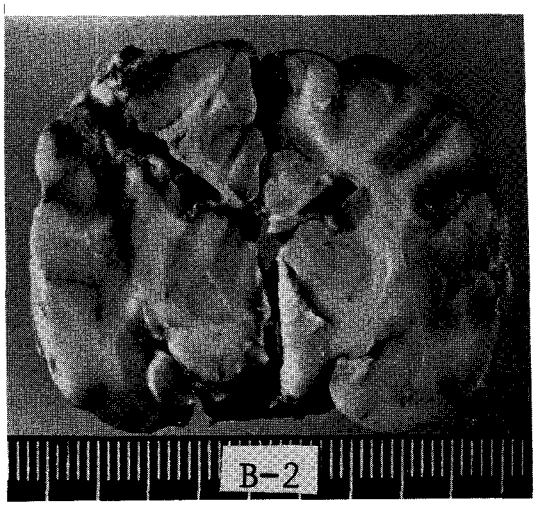

Fig. 5. Gross photograph of canine brain at 7 days after 42.5 C hyperthermia for 50 minutes. Marked necrotic change on implanted canine brain.

With the RF electrode needles, the current density deposited near the needles is high, although it is reasonably constant along the centerline between the two rows of implants. Strohbehn reported the maximum power density is at the surface of the electrode and falls off rapidly with a $1/r^2$ dependence, where r is the distance from the electrode[1]. The major point is that, if the temper-

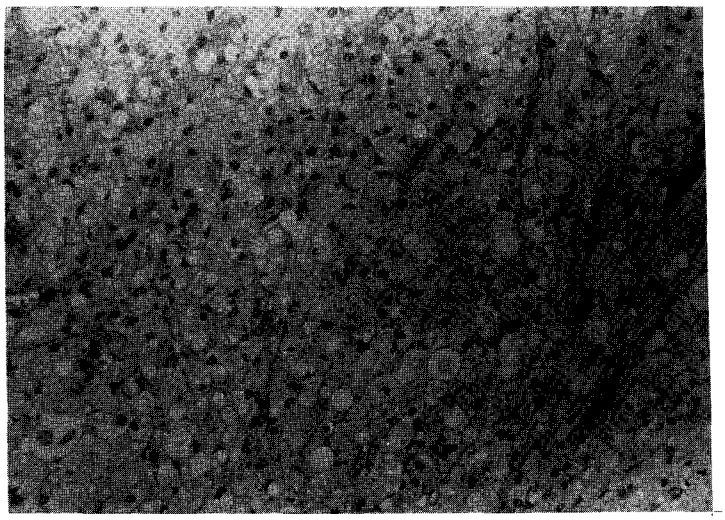

Fig. 6. Light microscopic photograph of canine brain at 7 days after 42.5 C hyperthermia for 50 minutes. The appearance of lipid-laden macrophages surrounding liquefactive necrotic area was demonstrated in all 3 sacrificed canine brains (H&E, 400).

ature at the electrodes are permitted to go high enough to produce acceptable therapeutic temperatures throughout the tumor, excellent thermometry data must be available in order to ensure against damaging normal tissue.

In this phantom study, the radial distribution of relative SAR around the four needles square array indicated reduction in absorbed power with increasing distance, We observed that the 1 cm square array showed 1.25 cm radius homogenous circular 90% relative SAR thermal distribution. Axially, absorbed power was greatest adjacent to the needle and decreased most rapidly distal to it. For clinical use, the multiple parallel square array would be needed for treatment. Moreover, the problem of steep temperature gradients demonstrated in the microwave antenna array could be overcome by grouping them into a parallel array with appropriate lengths. We concluded that if the electrodes are spaced about 1 cm apart and the voltage is adjusted to optimize the temperature distribution, reasonably good results should be achievable.

A number of groups have been using RF needle electrodes in the clinic. These reports demonstrate that RF electrode systems are feasible for clinical treatment of superficial tumors and could also be used for deep-seated tumors[10~13]. Many of these trials showed good short-term response to the treatemtn when used in conjunction with radiation therapy. Cosset et al. showed that reasonably uniform temperature distribution can be obtained when proper control of the voltage to the needles is used[5]. Unfortunately, a number of the other studies do not provide good temperature data; hence, it is not possible to judge how much of the tumor volume was brought to therapeutic temperatures. More long term clinical studies are needed with more attention to collecting adequate temperature data. In addition, there is room for further improvement in the engineering of these systems to provide more control to the temperature distribution throughout the tumor volume.

2. Thermal Injury in Normal Canine Brain Tissue

Hyperthermia has been shown to be effective against undervascularized tissues that have radioresistant hypoxic areas and are low in pH. Furthermore, this treatment modality has been shown to be synergistic with ionizing radiation. Since hyperthermia and radiation are interactive in their effect, this fact is the most convincing argument for the addition of hyperthermia treatment to the conventional brain tumor therapy[14~16]. Walker et al have demonstrated a positive doses-response correlation of these tumors after conventional teletherapy. However, doses higher than 60 Gy cause unacceptable radiation necrosis in the normal brain tissue[17]. If hyperthermia can be precisely delivered to the tumor region, the synergistic interaction of heat and radiation may extend the mean survival in these patients. Before localized hyperthermia can be used to treat malignant brain tumors, the tolerance of the normal brain must be thoroughly understood. Many experimental and clinical studies have demonstrated a role for hyperthermia in an animal brain model using microwave antenna arrays[18~20]. When hyperthermia is administered by interstitially implanted microwave antennas, the orientation and geometrical arrangement of the implant governs the distribution of absorbed microwave power and the resultant distribution of heat. Stanford groups has demonstrated that localized hyperthermia using either ultrasound(US) or microwave(MW) energy can cause significant injury to normal canine or feline brain tissues if temperatures exceed 42°C for 60 min of heating. These histological studies are essential to understanding heat-induced morphological changes in the central nervous system[21,22].

However, these studies were performed on acutely sacrificed animals and the late effects of thermal injury on normal brain tissue were not appreciated. The question remains whether the structural changes seen immediately after hating were reversible or permanent. Lyons et al demonstrated a significant linear dose-response correlation (mean lesion size versus thermal dose)[22]. Thermal damage as illustrated in their studies appears to be analogous to cerebral necrosis such as that caused by ischemic infarction. Early work by other investigators has demonstrated that the threshold for lesion production differs for various brain tissues. They suggested that brain tissue can be ranked from highest to lowest heat sensitivity as follows: neuron, myelin sheaths, axon cylinders, neuroglia and blood vessel elements. Therefore, these known differences warrant a long-term histopathological study of normal brain tissue after exposure to combination heat and radiation.

This study was initiated to determine the sequential neuropathological changes that occur as a function of heat damage over time in normal brain tissue. Thermal damage, as illustrated in this study, also appears to be analogus to cerebral necrosis such as that caused by ischemic infarction. Late

changes are characterized by mild gliosis in the surrounding viable brain tissue. In general, the histopathological disease (infarction) or thermal insult are characterized by a precise reparative phenomenon that evolves with time. However, thermal damage caused by a RF needle implantation dose not result in significant intracranial hemorrhage. A significant dose-response correlation was warranted.

REFERENCES

1. **Strohbehn JW:** Temperature distribution from interstitial RF electrode hyperthermia systems: Theoretical predictions. Int J Rad Oncol Biol Phys 9:1655-1667, 1983
2. **Arcangeli G, Cividalli A, Nervi C, et al:** Tumor control and therapeutic gain with different schedules of combined radiotherapy and local external hyperthermia in huma cancer. Int J Rad Oncol Biol Phys 9:1125-1134, 1983
3. **Dewhirst MW, Sim DA, Sapareto SA, et al:** The importance of minimum tumor temperature in determining early and long-term response of spontaneous pet animal tumors to heat and radiation. Cancer Res 44:43-50, 1984
4. **Scott RS, Johnson RJ, Story KV, et al:** Local hyperthermia in combination with definitive radiotherapy: Increased tumor clearance, reduced recurrence rate in extended follow-up. Int J Rad Oncol Biol Phys 10:2119-2123, 1984
5. **Cosset JM, Dutreix J, Dufour J, et al:** Combined interstitial hyperthermia and brachytherapy: Institute Gustabe Roussy Technique and Preliminary results. Int J Rad Oncol Biol Phys 10:307-312, 1984
6. **Brezovich IA, Atkinson WJ, Lilly MB:** Local hyperthermia with interstitial techniques. Cancer Res. (Suppl.) 44:4752s-4756s, 1984
7. **Mechling JA, Strohbehn JW:** A Theoretical comparision of the temperature distributions produced by three interstitial hyperthermia systems. Int J Rad Oncol Biol Phys 12:2137-2149, 1986
8. **Hand JW, Haar G:** Heating techniques in hyperthermia: I. Introduction and assessment of techniques. Brit J Radiol 54:443-446, 1981
9. **Gerner EW, Connor WG, Boone MLM, et al:** The potential of localized heating as an adjunct to radiation therapy. Radiology 116:433-439, 1975
10. **Emami B, Marks J, Perez C, et al:** In hyperthermic oncology, Summary papers, (J Overgarard, ed.). London: Taylor & Francis, p 583, 1984
11. **Joseph CD, Astrahan M, Lipsett J, et al:** Interstitial hyperthermia and Interstitial Iridium-192 implantation: A Technique and preliminary results. Int J Rad Oncol Biol Phys 7:827-833, 1981
12. **Manning MR, Cetas TC, Miller RC, et al:** Clinical hyperthermia: Results of a phase I trial employing hyperthermia alone or in combination with external beam or interstitial radiotherapy. Cancer 49: 205-216, 1982
13. **Vora N, Forell B, Joseph C, et al:** Interstitial implant with interstitial hyperthermia. Cancer 50:2518 -2523, 1982
14. **Silberman AW, Morgan DF, Storm FK, et al:** Combination radiofrequency hyperthermia and chemotherapy(BCNU) for brain malignancy. J Neuro-Oncol 2:19-28, 1984
15. **Roberts DW, Coughlin CT, Wong TZ, et al:** Interstitial hyperthermia and iridium brachytherapy in the teratment of malignant gliomas: A phase I clinical trial. J Neurosurg 64:581-587, 1986
16. **Salcman M, Samaras GM:** Interstital microwave hyperthermia for brain tumors: Results of a phase I clinical trial. J Neuro-Oncol 1:225-236, 1984
17. **Walker MD, Strike TA, Sheline LA:** An analysis of dose-effect relationships in the radiotherapy of malignant gliomas. Int J Rad Oncol Biol Phys 5: 1725-1731, 1979
18. **Koh KH, Cho CK, Park YH, et al:** The study of standardization of temperature distribution of interstitial hyperthermia-In phantoms and living cat's brain tissue (normal tissue). J Korean Soc Ther Radiol: Vol. 8, No. 1, 7-15, 1990
19. **Sneed PK, Matsumoto K, Stakuffer PR, et al:** Interstitial microwave model hyperthermia in a canine brain model. Int J Rad Oncol Biol Phys 12:1887 -1897, 1986
20. **Denman DL, Elson HR, Lewis GC, et al:** The distibution of power and hear produced by interstitial microwave antenna arrays: I. Comparative phantom and canine studies. Int J Rad Oncol Biol Phys 14:127-137, 1988
21. **Dewey WC, Hopwood LE, Sapareto SA, et al:** Cellular responses to combinations of hyperthermia and radiation. Radiology 12:463-474, 1977
22. **Lyons BE, Obana WG, Borcich JK, et al:** Chronic histological effects of ultrasonic hyperthermia on normal feline brain tissue. Rad Res 106:234-251, 1986

= 국문초록 =

8 MHz 라디오파를 이용한 자입식 온열치료

— 조직등가물질을 통한 온도분포 및 개 뇌실질의 조직병리 변화에 관한 연구—

연세대학교 의과대학 치료방사선과학교실, 신경외과학교실*, 해부병리학과학교실**

이형식 · 추성실 · 성진실 · 서창옥 · 김귀언 · 노준규
김영수* · 김선호* · 정상섭* · 한은경** · 김태승**

8 MHz 라디오파를 이용한 자입식 온열치료를 위한 기초실험의 일환으로 조직등가물을 이용하여 다양한 needle electrode의 배열을 통한 적정 온도분포를 규명하고자 하였고, 직접 개의 뇌실질에 자입 온열요법을 시도하여 이에 따른 조직 병리학적 소견을 관찰하고자 하였다. 조직등가물 실험에서 저자들은 needle electrode 1 cm 간격의 정방형 배치에서 횡단면상 90% relative SAR 분포가 약 1. 25 cm 반경의 균일한 원형으로 관찰됨을 알 수 있었고 종단면상 needle electrode의 길이에 따라 균일한 온도분포가 이루어짐을 관찰할 수 있었다. 정상 개의 뇌실질에 자입하여 직접 정방형의 중심을 43°C로 유지하며 50분간 온열요법을 시행한 후 관찰한 조직병리학적 소견은 liquefactive necrosis, pyknosis of neuronal element 및 polymorphonuclear leukocytes들이 회백질에서 급성기에 관찰되었고 liquefactive necrosis 주위에 lipid-laden macrophage들이 관찰됨이 공통적인 특징이었으며 후기 변화로 괴사조직 주위로 신경교세포의 증식이 관찰되었다